Published in final edited form as:
J Opt Soc Am A Opt Image Sci Vis. 2013 November 1; 30(11): 2401–2408.

Modeling lateral geniculate nucleus response with contrast gain control. Part 1: Formulation

Davis Cope[1], **Barbara Blakeslee**[2], and **Mark E. McCourt**[2,*]

[1]Department of Mathematics NDSU Dept #2750, North Dakota State University PO Box 6050, Fargo, ND 58108-6050, USA

[2]Center for Visual and Cognitive Neuroscience, Department of Psychology NDSU Dept #2765, North Dakota State University PO Box 6050, Fargo, ND 58108-6050, USA

Abstract

A class of models for lateral geniculate nucleus (LGN) ON-cell behavior is proposed. The models consist of a linear filter with divisive normalization by root mean square local contrast and include an intrinsic noise density parameter. The properties of these models are shown to match observed LGN behavior: (1) a linear response to low magnitude stimuli; (2) a linear response without saturation (*luxotonic behavior*) for zero contrast stimuli (homogeneous fields) with increasing magnitude; (3) response saturation for non-zero contrast stimuli with increasing magnitude. The models possess an intrinsic scale for signal-to-noise ratio (SNR). The models show under- and super-saturation, as well as saturation, for sinusoidal grating stimuli with increasing contrast and predict that different SNR regimes will cause a single neuron to show different contrast response curves. A companion paper (Cope, Blakeslee and McCourt, 2013) provides a detailed analysis of the full nonlinear response for sinusoidal grating stimuli and circular spot stimuli.

1. Introduction

The purpose of this paper is to introduce a general class of nonlinear analytical models which capture the full range of behavior that is experimentally observed for neurons in the lateral geniculate nucleus, in particular, both luxotonic and saturated responses. This paper formulates these models and derives their key properties. A companion paper (Cope, Blakeslee and McCourt [1]) provides a detailed analysis of a five-parameter model of this type, and selected results from that companion paper are included here for illustration.

The lateral geniculate nucleus (LGN) is a thalamic visual relay nucleus which receives input from the retina and projects to the primary visual cortex. Receptive fields of LGN neurons have roughly circular symmetry and exhibit center-surround antagonism, where the response of the center region to light can be either excitatory (ON-center) or inhibitory (OFF-center) [2,3]. Neurons in the LGN exhibit a number of canonical properties which analytical models of their behavior should reflect. The first of these properties is the saturation of response

*Corresponding author: Mark.Mccourt@ndsu.edu.

Commercial relationships: none.

with increasing stimulus contrast, i.e., contrast gain-control [4–12]. A behavior related to response saturation is that some LGN (and cortical) neurons exhibit response super-saturation [5, 13], where response actually decreases with increasing stimulus contrast. A third property is that the response of LGN cells increases monotonically with increasing luminance for homogeneous fields, that is, they exhibit *luxotonic behavior* over many orders of magnitude [2,3,14–26].

This seeming contradiction, that LGN cells show both non-saturation (luxotonic behavior for homogeneous fields) and saturation for other stimuli, motivates this paper. Furthermore, when homogeneous stimuli of increasing magnitude cause the LGN response to increase without saturation, that increasing LGN response is the input for simple cells in the primary visual cortex, yet simple cells give a zero response to homogeneous stimuli. This fact suggests that luxotonic behavior may give special insight into the interaction between LGN cells and simple cells and thus further motivates the formulation of an LGN model that can reproduce luxotonic behavior.

Finally, analytical models should embody the fact that whereas frequency-domain properties of LGN responses (such as optimal spatial frequency, spatial frequency and orientation bandwidth) are relatively invariant with grating contrast [27], space-domain properties (such as the diameter of the circular spot stimulus eliciting maximal response) are not invariant, but depend on spot contrast [15].

Section 2 formulates a general class of models, which consist of a *linear filter* with *divisive normalization* by a root mean square *local contrast* and include an *intrinsic noise density*. These models address the ON-center response. The general formulation derives properties of this class of models which are independent of particular choices for the receptive field function defining the linear filter and the gain control function (gain pool) defining the local contrast weight. That is, this class of models is shown to be *structurally stable*. The properties include an intrinsic scale for measuring signal-to-noise ratio (SNR), response saturation, luxotonic behavior, and a mechanism for super-saturation. We do not know of any other model for LGN neurons that claims to produce this range of observed LGN behavior, that is, both saturating and luxotonic responses.

Section 3 provides illustrative examples of the response to sinusoidal grating stimuli, which are chosen as a familiar class of stimuli for checking the behavior of the model. These examples are drawn from the work of the companion paper [1], which studies a five-parameter model of this class consisting of a difference-of-Gaussians receptive field function [28, 29] and a Gaussian gain pool and the full nonlinear response to sinusoidal grating and circular spot stimuli. An unexpected result follows from the model's intrinsic scale for SNR, which provides a means of studying saturation behavior as SNR varies. It is known that contrast response curves can show under-saturation, saturation, and super-saturation, but the reason for this variation is unknown. One hypothesis is that the different behaviors result from different types of neurons. Our model shows that a single LGN neuron can show all three types of contrast response curve, the types being associated with different SNR regimes. The implication is that the contrast response curve shown by a neuron is determined by the stimulus magnitude (relative to the level of intrinsic noise in the neuron).

Related modeling

The general form of a linear filter divided by a root mean square gain control is used in various LGN models. The use of a difference of circular Gaussians for the receptive field function defining the linear filter is a well established choice [8, 28–30]. Quadratic gain control mechanisms vary in details and the differences are sometimes crucial. For example, Mante et al. [30] omit an additive constant which appears in our formulation as the (strictly positive) intrinsic noise density parameter. Its omission means that gain control for a homogeneous stimulus would involve division by zero. Inclusion of such a parameter was not crucial in [30] because that paper analyzed natural scenes, which are typically nonhomogeneous (except perhaps for sky [31]), but its inclusion is absolutely necessary for our purposes. Bonin et al. [8] use a root mean square gain control mechanism that involves, as a partial step, averaging the stimulus over a grid of fifty difference-of-Gaussians filters for the purpose of simulating gain control as originating at the retinal level. The models of [30] and [8] do not consider luxotonic behavior. We present our class of models as the simplest formulation that can reproduce both saturated and luxotonic responses. This class of models has divisive normalization form, which Carandini and Heeger [32] have proposed as a “canonical neural computation”. We note that their general definition of the divisive normalization form includes an additive constant, similar to our intrinsic noise density parameter ν_G (see Section 2), and that the definition of signal-to-noise ratio (SNR) in terms of ν_G presented in this paper would hold for divisive normalization in general. The occurrence of this definition of SNR within our models leads to the recognition that different types of saturation phenomena are associated with corresponding SNR regimes. In fact, it allows us to frame a new hypothesis to explain the occurrence of different types of saturation in contrast response curves (see Section 3 and the discussion accompanying Figure 5). The use of this definition for SNR may be similarly productive for other divisive normalization models as well.

2. A general class of models for LGN ON-center cell response

This section formulates a general class of models for the response of a single LGN ON-center cell to general stimulus patterns. This class of models is shown to possess the following properties: (1) an intrinsic scale for defining a signal-to-noise ratio (SNR); (2) the response reduces to the linear field response for small SNR; (3) response saturation with respect to increasing SNR with the sole exception of homogeneous field stimuli; (4) nonsaturation of the response to a homogeneous field stimulus (luxotonic behavior); (5) a general mechanism for super-satuation. The general formulation of this section leaves the choice of receptive field function and the gain control function arbitrary to emphasize that the properties do not depend on special choices for these functions, that is, the general class of models proposed here is structurally stable with respect to the properties. Section 3 gives a specific formulation as a basis for discussion and examples.

General formulation

The *total model response* LGN[P] for the LGN ON-center cell to a stimulus pattern $P(x)$ has units [spikes/sec] and is modeled as

$$\mathrm{LGN}[P] = \nu_{\mathrm{LGN}} \,\mathrm{Pos}\left(\frac{R[P]}{G[P]}\right) \quad (1)$$

where $\nu_{\mathrm{LGN}} > 0$ is an *output factor* [spikes/sec] which compensates for normalizations that occur in the model, $R[P]$ is the *linear field response*, $G[P]$ is the *gain control response*, the ratio $R[P]/G[P]$ is dimensionless, and $P(\vec{x})$ is the *stimulus pattern*, a nonnegative function with units [spikes/ (sec · deg^2)] which represents the stimulus pattern as encoded by retinal ganglion cell activity. The reader should note, therefore, that the spatial patterns taken as input to the model consist of "neural images" [33], that is, patterns of neural activity, and not distributions of retinal light intensity. We make the customary assumption that the retinal ganglion cell input to the LGN is proportional to the stimulus magnitude. The visual field is the plane with coordinates (x_1, x_2), briefly, $\vec{x}$ and patterns are nonnegative bounded functions on the plane.

The linear field response $R[P]$ with units [spikes/ (sec · deg^2)] to a stimulus pattern $P(\vec{x})$ is modeled as

$$R[P] := \int_{\mathbb{R}\times\mathbb{R}} R\left(\vec{y}\right)\, P\left(\vec{y}\right)\, d\,\vec{y} \quad (2)$$

The *linear field function* $R(\vec{x})$ has units [deg^{-2}] and is assumed absolutely integrable. The dimensionless *balance* is the volume associated with R and defines the *balance parameter* β_{CS} by:

$$\int_{\mathbb{R}\times\mathbb{R}} R\left(\vec{x}\right)\, d\,\vec{x} = 1 - \beta_{CS} \quad (3)$$

The balance is required to be nonnegative, that is, $\beta_{\mathrm{CS}} \leq 1$, to agree with observed LGN properties. The majority of LGN cells are found to possess stronger center versus surround responses, so that normally $\beta_{\mathrm{CS}} < 1$. Published estimates of β_{CS} in LGN include the following: Macaque [4] [average $\beta_{\mathrm{CS}} = 0.65$]; [34] [average $\beta_{\mathrm{CS}} = 0.60$ and 0.68 (M-cells); 0.54 and 0.52 (P-cells)]; [23] [average $\beta_{\mathrm{CS}} = 0.82$ (M-cells) and 0.60 (P-cells)]; Galago [35] [average $\beta_{\mathrm{CS}} = 0.87$]; marmoset [36] [average $\beta_{\mathrm{CS}} = 0.64$]; [37] [average $\beta_{\mathrm{CS}} = 0.57$ (K-cells)]; Aotus [38] [average $\beta_{\mathrm{CS}} = 0.92$ (M-cells) and 0.64 (P-cells)]; [39] [median $\beta_{\mathrm{CS}} = 0.77$ (K-cells), 0.75 (M-cells), and 0.75 (P-cells)]; cat [40] [average $\beta_{\mathrm{CS}} = 0.95$]; and mouse [41] [average $\beta_{\mathrm{CS}} = 0.60$].

The gain control response $G[P]$ with units [spikes/ (sec · deg^2)] to a stimulus pattern $P(\vec{x})$ is modeled as

$$G[P] := \left(\int_{\mathbb{R}\times\mathbb{R}} G\left(\vec{y}\right)\, \left(P\,\left(\vec{y}\right) - \mu_{\mathrm{G}}[P] + \nu_{\mathrm{G}}\right)^2 d\,\vec{y}\right)^{1/2} \quad (4)$$

where the *local pattern mean* $\mu_{\mathrm{G}}[P]$ with units [spikes/ (sec · deg^2)] is given by

$$\mu_{\mathrm{G}}[P] := \int_{\mathbb{R}\times\mathbb{R}} G\,\left(\vec{y}\right)\, P\left(\vec{y}\right)\, d\,\vec{y} \quad (5)$$

The *gain control function* $G(\vec{x})$ has units [deg^{-2}] and is assumed to be nonnegative and normalized to unit volume:

$$\int_{\mathbb{R}\times\mathbb{R}} G\left(\vec{x}\right)\, d\,\vec{x} = 1 \quad (6)$$

The final parameter, $\nu_G > 0$, is a normalized *intrinsic noise density* with units [spikes/ (sec · deg^2)]. It represents a measure of intrinsic noise in the neuron and is assumed constant. The noise is added to the pattern within the gain control mechanism. Normalization of the gain control function to unit volume implies that both ν_G (and the pattern P) have normalized (scaled) values. The following identity,

$$\begin{aligned} Var_G[P]: &= \int_{\mathbb{R}\times\mathbb{R}} G\left(\vec{y}\right)\, \left(P\left(\vec{y}\right) - \mu_G[P]\right)^2 d\,\vec{y} \\ &= \int_{\mathbb{R}\times\mathbb{R}} G\left(\vec{y}\right)\, P\left(\vec{y}\right)^2 d\,\vec{y} - \mu_G[P]^2 \end{aligned} \quad (7)$$

where the second form follows because $G(\vec{x})$ has unit volume, allows the gain control response to be expressed as:

$$G[P] = \left(Var_G[P] + \nu_G^2\right)^{1/2} \quad (8)$$

The gain control response thus corresponds to the standard deviation of the stimulus pattern with the gain control function as a weight and the addition of intrinsic noise. Notice the gain control response is necessarily positive.

Saturation in the general model

LGN cells can show *response saturation*, that is, a stage at which increasing the stimulus magnitude produces no further increase in response, and even *super-saturation*, a stage at which increasing the stimulus magnitude reduces the response. Such behavior is highly nonlinear, and we will now show that such response saturation is a general property of the model presented above.

Notice that any stimulus pattern can be expressed as the product of a scaling factor and a fixed dimensionless component:

$$P\left(\vec{x}\right) = \nu_{MAG}\, p\left(\vec{x}\right) \quad (9)$$

where $\nu_{MAG} \geq 0$ is some measure of the magnitude of the stimulus pattern and has units [spikes/ (sec · deg^2)]. The specific definition of ν_{MAG} will depend on the class of stimuli, for example, ν_{MAG} may be the maximum value of the pattern P, or it may be the maximum value or mean value of some family of patterns which include P. Once ν_{MAG} is defined, $p(\vec{x})$ becomes the dimensionless case of the pattern. The definitions above give

$$\begin{aligned} R[P] &= \nu_{\mathrm{MAG}} R[p] \\ \mathrm{Var}_{\mathrm{G}}[P] &= \nu_{\mathrm{MAG}}^2 \mathrm{Var}_G[p] \\ G[P] &= \nu_{\mathrm{G}} \left(1 + \frac{\nu_{\mathrm{MAG}}^2}{\nu_{\mathrm{G}}^2} \mathrm{Var}_{\mathrm{G}}[p]\right)^{1/2} \end{aligned} \quad (10)$$

The *normalized total response* corresponding to Eq. (1) can then be written as the quotient of the *normalized linear field response* $R[P]/\nu_G$ and the *normalized gain control response* $G[P]/\nu_G$, that is, using the fact that the gain control response is necessarily positive:

$$\begin{aligned} \frac{\mathrm{LGN}[P]}{\nu_{\mathrm{LGN}}} &= \frac{\mathrm{Pos}\left(R[P]/\nu_{\mathrm{G}}\right)}{G[P]/\nu_{\mathrm{G}}} \\ \frac{G[P]}{\nu_{\mathrm{G}}} &= \left(1 + \frac{\nu_{\mathrm{MAG}}^2}{\nu_{\mathrm{G}}^2} \mathrm{Var}_{\mathrm{G}}[p]\right)^{1/2} \end{aligned} \quad (11)$$

This formula has three important implications. First, the parameter ν_G appears *only* in the dimensionless ratio ν_{MAG}/ν_G, which will be designated the *signal-to-noise ratio* (SNR). In this way, ν_G sets an inherent scale for the strength of the stimulus pattern as input to the LGN cell. Second, for small values of the SNR ν_{MAG}/ν_G, the total response reduces to the linear field response. Third, for $\mathrm{Var}_G[p] \neq 0$, the limit

$$\begin{aligned} \lim_{\frac{\nu_{\mathrm{MAG}}}{\nu_{\mathrm{G}}} \to \infty} \frac{\mathrm{LGN}[P]}{\nu_{\mathrm{LGN}}} &= \lim_{\frac{\nu_{\mathrm{MAG}}}{\nu_{\mathrm{G}}} \to \infty} \mathrm{Pos}\left(\frac{\frac{\nu_{\mathrm{MAG}}}{\nu_{\mathrm{G}}} R[p]}{\left(1 + \frac{\nu_{\mathrm{MAG}}^2}{\nu_{\mathrm{G}}^2} \mathrm{Var}_{\mathrm{G}}[p]\right)^{1/2}}\right) \\ &= \mathrm{Pos}\left(\frac{R[p]}{\mathrm{Var}_{\mathrm{G}}[p]^{1/2}}\right) \geq 0 \end{aligned} \quad (12)$$

exists and implies that LGN[*P*] will approach a nonnegative limiting response as $\nu_{MAG}/\nu_G \to \infty$, that is, that the response will *saturate* as a general effect of increasing the stimulus magnitude, ν_{MAG}.

There is an important exception to the observation that responses will generally saturate as stimulus magnitudes increase. For the homogeneous stimulus $P(x) = \nu_P$, the receptive field response from Eq. (2) is $\nu_P (1 - \beta_{CS})$, where normally $1 - \beta_{CS} > 0$, and the variance from Eq. (7) is zero, giving the total response

$$\frac{\mathrm{LGN}[\nu_{\mathrm{P}}]}{\nu_{\mathrm{LGN}}} = \frac{\nu_{\mathrm{P}}}{\nu_{\mathrm{G}}} (1 - \beta_{CS}) \quad (13)$$

This response simply increases as ν_P/ν_G increases, and saturation does *not* occur. We note that this exceptional behavior of the LGN response to a homogeneous stimulus has been observed experimentally, where luxotonic behavior has been reported in LGN of the following: Macaque [15,17,19,21–23,26]; squirrel monkey [14]; tree shrew [25]; cat [2,3,16,20]; and squirrel [24].

A mechanism for super-saturation in the general model

The existence of a nonsaturating stimulus provides a possible general mechanism for *super-saturation*, a decrease in response as the stimulus magnitude increases. Consider a

nonhomogeneous stimulus *A*. Assume that the magnitude of *A* has been scaled up sufficiently that the corresponding response has saturated at some level A_1. Assume *B* is a homogeneous field stimulus that has been scaled sufficiently to give a response $B_1 > A_1$. Now scale *A* further to insure that it has a magnitude larger than *B*. This new scaling does not change the value A_1 because that is the saturated value. Take a parameterized combination of *A* and *B* in terms of *c* such that $c = 0$ gives *A* alone, that is, a large stimulus, and $c = 1$ gives *B* alone, that is, a smaller stimulus. But the response at $c = 0$ is A_1 and the response at $c = 1$ is $B_1 > A_1$. Super-saturation has occurred.

3. Illustrative responses to sinusoidal grating stimuli

This section gives a specific formulation for an LGN ON-center neuron of the type described in Section 2. The formulation is the five-parameter model studied in our companion paper [1], and illustrative results here are taken directly from that paper. A specific formulation is necessary to provide computational results. The results shown here are for sinusoidal grating stimuli, which are chosen as the simplest and perhaps most familiar stimuli to provide test cases for the model. Figure 1 shows cross-sections of receptive field functions. Figures 2, 3, 4 illustrate the linear field, gain control, and total responses of the model to sinusoidal grating stimuli. Figure 5 illustrates contrast response curves generated by the model for sinusoidal grating stimuli and also illustrates luxotonic behavior in the model. The figure is particularly interesting because it illustrates an explanation provided by our models for experimentally observed variations in contrast response curves. See the discussion in regard to the figure. Figure 6 shows a response surface as a function of contrast and frequency for sinusoidal grating stimuli. The plot illustrates that the optimal frequency for the nonlinear response can remain fixed at the linear response value as contrast varies. The companion paper presents a detailed analysis of the nonlinear response of the model and determines conditions under which an optimal frequency exists and remains stable. The figure illustrates a stable case.

Specification of field functions

The linear field function is the customary difference of unit circular gaussians field function:

$$R\left(\vec{x}\right) := \frac{1}{2\pi\sigma_{\mathrm{C}}^2}\exp\left(-\frac{x_1^2+x_2^2}{2\sigma_{\mathrm{C}}^2}\right) - \frac{\beta_{CS}}{2\pi\sigma_{\mathrm{S}}^2}\exp\left(-\frac{x_1^2+x_2^2}{2\sigma_{\mathrm{S}}^2}\right) \quad (14)$$

The parameters consist of a center sigma, $\sigma_{\mathrm{C}} > 0$ [deg], a surround sigma, $\sigma_{\mathrm{S}} > 0$ [deg], and a balance parameter, $0 < \beta_{\mathrm{CS}} \leq 1$ [dimensionless], which are independent. The balance parameter is consistent with the definition of balance in Eq. (3). Figure 1 shows cross-sections of four linear field functions and a gain control function (multiplied by 10 to aid visualization).

The gain control field function is a unit circular gaussian:

$$G\left(\vec{x}\right) := \frac{1}{2\pi\sigma_{\mathrm{G}}^2}\exp\left(-\frac{x_1^2+x_2^2}{2\sigma_{\mathrm{G}}^2}\right) \quad (15)$$

Its single parameter is the gain sigma, $\sigma_G > 0$ [deg]. Figure 1 also shows a cross-section of such a gain control field function.

Conditions on the linear field function typically include:

(a) the field function *R* is positive at the origin (holds iff $\beta_{CS}\frac{\sigma_C^2}{\sigma_S^2} < 1$);

(b) a *zero-crossing radius* $r = \rho_0$ exists (holds iff $\exp\left(\frac{\rho_0^2}{2\sigma_S^2} - \frac{\rho_0^2}{2\sigma_C^2}\right) = \beta_{CS}\frac{\sigma_C^2}{\sigma_S^2}$);

(c) total volume associated with the field function *R* is nonnegative (holds iff $\beta_{CS} \leq 1$).

In condition (b), the value $r = \rho_0$ is unique. It is the radius of the excitatory center region of the (ON-center) LGN cell (i.e., distance to the zero-crossing). We assume these conditions and note that they are equivalent to the following relations, which describe the exact extent of σ_C, σ_S, β_{CS}-space in which the parameters can lie:

$$0 < \sigma_C < \sigma_S \text{ and } 0 < \beta_{CS} \leq 1 \quad (16)$$

Sinusoidal grating stimuli

These stimuli have the general form

$$P\left(\vec{x}\right) = \nu_P\left(1 + c_P cos\left(2\pi s_P\left(\vec{d}\,(\alpha_P)\cdot\vec{x}\right) - \phi_P\right)\right) \quad (17)$$

where the subscript P is used for pattern parameters. The main parameters for our discussion are the measure of stimulus magnitude, ν_P [spikes/ (sec · deg^2)], the spatial frequency, s_P [cycle/deg], and the dimensionless Michelson contrast c_P of the sinusoidal grating. These parameters satisfy $\nu_P \geq 0$, $s_P > 0$, and $-1 \leq c_P \leq +1$. For a given grating, the magnitude lies between the bounds $\nu_P(1 \pm |c_P|)$. The direction of the grating, α_P, is orthogonal to its orientation, and is determined by $\vec{d}\,(\alpha_P)\cdot\vec{x} = cos(\alpha_P)\,x_1 + sin(\alpha_P)\,x_2$. The LGN model response will be independent of grating direction, α_P, due to the circular symmetry of its receptive field structure. Grating motion in a given direction is achieved by making grating phase, φ_P, time-dependent. Electrophysiological experiments typically involve drifting gratings across the LGN receptive field while recording spike activity, and the maximum discharge rate per stimulus period can be recovered from the post-stimulus time histogram. The corresponding maximum response of the model,

$$\left(\frac{\mathrm{LGN}[P]}{\nu_G}\right)_{max} := \max_{\phi_P}\left(\frac{\mathrm{LGN[P]}}{\nu_G}\right) \quad (18)$$

as well as the related quantities $(R[P]\nu_G)_{max}$ and $(G[P]\nu_G)_{min}$, are found explicitly in our companion paper [1] and are used in reporting results here. Altogether, the key parameters for sinusoidal grating stimuli are stimulus magnitude ν_P, spatial frequency s_P, contrast c_P, and SNR = ν_P/ν_G.

Illustration of linear field response

Figure 2 shows plots of the linear field response versus spatial frequency at fixed contrast. The response is shown for a single linear field function, that is, a single set of parameters σ_C, σ_S, β_{CS}. The response shows strong band-pass behavior and scales linearly with the SNR, as shown for the sample values $\nu_P/\nu_G = 1, 2, 4, 8$. For the linear response, the optimal frequency does not change with SNR.

Illustration of gain control response

Figure 3 shows plots of the gain control response versus spatial frequency at fixed contrast. The response is shown for a single gain control function, that is, a single value for the parameter σ_G, and for the same four SNR values as Figure 2. Notice the gain control value varies from the fixed value one at zero frequency (that is, no gain control) to values proportional to the SNR at high frequency (that is, full gain control). Notice the optimal frequency of the linear response lies well inside the plateau of full gain control at all SNR levels. We realize that, in the real visual system, gain control must decrease with increasing spatial frequency, due to optical demodulation and the finite dimensions of the pooling sub-units, but including this feature is not critical for our present purposes.

Illustration of total response

Figure 4 shows plots of the total response when the responses of Figures 2 and 3 are combined, that is, a strong bandpass linear response with gain control applied. Notice that the response at zero frequency is unbounded (illustrating luxotonic response), that response saturation is occurring at other frequencies, and that the optimal frequency of this nonlinear response remains essentially unchanged, namely, the same value as the optimal frequency for the linear response. This unchanged optimal frequency is a consequence of the fact that the optimal frequency lies well inside the plateau of full gain control.

Illustration of under-saturation, saturation, and super-saturation with contrast

Figure 5 shows saturation effects in contrast response curves plotted for the total response at the same four SNR values used in the preceding figures. In other words, the model implies that a single LGN neuron, as defined by the particular receptive field and gain control parameters of the preceding figures, can generate different types of contrast response curves. The type of curve depends on the SNR level. Notice that it is possible to recognize and study this behavior because the model has an intrinsic definition of SNR. An alternate hypothesis for the occurrence of different types of contrast response curves is that they are generated by different types of neurons. Our model presents the experimentally testable hypothesis that such under-saturation, saturation, super-saturation in contrast response curves is a consequence of the SNR regime, not a consequence of the LGN cell itself.

Illustration of combined contrast and frequency response

Figure 6 shows a plot of the total response versus contrast and spatial frequency. The SNR value is $\nu_P/\nu_G = 4$, corresponding to the straightforward contrast saturation case of Figure 5. The surface shows such various effects as luxotonic behavior at zero frequency, contrast saturation, and the stability of the optimal spatial frequency with respect to contrast.

4. Summary

This paper presents a general class of models for LGN ON-center behavior. These models are intended to reproduce experimentally observed saturation behavior associated with LGN neurons and thus are necessarily nonlinear. Relevant points include:

(1) The models allow arbitrary patterns as input stimuli. That is, the models can be applied to arbitrary stimuli, such as sinusoidal gratings, circular spots, cross-oriented gratings, or more general patterns. In particular, there is no restriction on the magnitude of the stimulus. Consequently, saturation effects can be derived as the limiting response to indefinitely increasing stimulus magnitudes.

(2) The models consist of a linear filter with divisive normalization by a gain control mechanism, namely, a root mean square local contrast with an intrinsic noise density parameter ν_G.

(3) In these models, the intrinsic noise density ν_G is taken to be a fixed value reflecting an aspect of the LGN neuron. As shown in Section 2, only the ratio ν_{MAG}/ν_G, where ν_{MAG} is a measure of stimulus magnitude, appears in the response. This ratio provides an intrinsic scale for the signal-to-noise ratio (SNR). The SNR provides a means of systematically studying saturation levels and corresponding effects.

(4) The models act as linear filters for low magnitude stimuli, that is, for small SNR, in agreement with experimentally observed behavior for LGN ON-center neurons.

(5) The models show two seemingly contradictory responses:

- **(a)** saturation (a limiting value for response to increasing SNR) for nonhomogeneous stimuli;
- **(b)** non-saturation (an indefinitely increasing response to increasing SNR) for homogeneous stimuli.

These responses are experimentally observed in LGN neurons, where (b) is known as luxotonic behavior. We do not know of any other model for LGN neurons that claims to produce this range of observed LGN behavior, that is, both saturating and non-saturating responses.

(6) The models provide a simple explanation for super-saturated behavior (an eventually decreasing response to increasing stimulus magnitude) in LGN ON-center neurons. This explanation is experimentally testable.

(7) The models imply that:

- **(a)** LGN ON-center neurons can show under-saturation, saturation, and super-saturation in contrast response curves;
- **(b)** a single neuron can show all three types of contrast response curves; and

(c) the type of contrast response curve depends on the SNR regime of the stimulus.

This implication is experimentally testable. We do not know of any other model for LGN neurons that predicts different types of contrast response curves for a single neuron nor of any model that implies the different types are the result of the SNR regime of the stimulus.

(8) The models form a general class in the sense that the properties above (with the possible exception of (7), which is based on results from the specific five-parameter case of Section 3 and the companion paper) are independent of particular choices for the receptive field function defining the linear filter and the gain pool function defining the gain control mechanism. That is, the class of models introduced here is structurally stable in the sense that their properties continue to hold even if different researchers make different choices for the receptive field or gain pool functions.

Acknowledgments

This work was supported by grant NIH P20 GM103505 from the National Institute for General Medical Sciences (NIGMS), a component of the National Institutes of Health (NIH). The contents of this report are solely the responsibility of the authors and do not necessarily reflect the official views of the NIH or NIGMS.

References

1. Cope D, Blakeslee B, McCourt ME. Modeling lateral geniculate nucleus response with contrast gain control. Part 2. Analysis. submitted.
2. Hubel DH. Single unit activity in the lateral geniculate body and optic tract of unrestrained cats. J. Physiol. (London). 1960; 150:91–104. [PubMed: 14403680]
3. Hubel DH, Wiesel TN. Integrative action in the cat's lateral geniculate body. J. Physiol. (London). 1961; 155:385–398. [PubMed: 13716436]
4. Derrington AM, Lennie P. Spatial and temporal contrast sensitivities of neurons in lateral geniculate nucleus of macaque. J. Physiol. 1984; 357:219–240. [PubMed: 6512690]
5. Kaplan E, Purpura K, Shapley RM. Contrast affects the transmission of visual information through the mammalian lateral geniculate nucleus. J. Physiol. 1987; 391:267–288. [PubMed: 2832591]
6. Kayser A, Priebe NJ, Miller KD. Contrast-dependent nonlinearities arise locally in a model of contrast-invariant orientation tuning. J. Neurophysiol. 2001; 85:2130–2149. [PubMed: 11353028]
7. Bonin, V.; Mante, V.; Carandini, M. Nonlinear processing in LGN neurons. In: Thrun, S.; Saul, L.; Schölkopf, B., editors. Advances in Neural Information Processing Systems. Vol. 16. MIT Press; Cambridge, MA: 2004. p. 1443-1450.
8. Bonin V, Mante V, Carandini M. The suppressive field of neurons in lateral geniculate nucleus. J. Neurosci. 2005; 25(47):10844–10856. [PubMed: 16306397]
9. Duong T, Freeman RD. Spatial frequency-specific contrast adaptation originates in primary visual cortex. J. Neurophysiol. 2007; 98:187–195. [PubMed: 17428911]
10. Mante V, Bonin V, Carandini M. Functional mechanisms shaping lateral geniculate responses to artificial and natural stimuli. Neuron. 2008; 58:625–638. [PubMed: 18498742]
11. Shou T, Li X, Zhou Y, Hu B. Adaptation of visually evoked responses of relay cells in the dorsal lateral geniculate nucleus of the cat following prolonged exposure to drifting gratings. Visual Neuroscience. 1996; 13:605–613. [PubMed: 8870219]
12. Solomon SG, Peirce JW, Dhruv NT, Lennie P. Profound contrast adaptation early in the visual pathway. Neuron. 2004; 42:155–162. [PubMed: 15066272]

13. Peirce JW. The potential importance of saturating and supersaturating contrast response functions in visual cortex. J. Vis. 2007; 7(6):13, 1–10. [PubMed: 17685796]
14. Jacobs GH, Yolton RL. Center-surround balance in receptive fields of cells in the lateral geniculate nucleus. Vis. Res. 1970; 10:1127–1144. [PubMed: 4995555]
15. Marrocco RT. Maintained activity of monkey optic tract fibers and lateral geniculate nucleus cells. Vis. Res. 1972; 12:1175–1181. [PubMed: 4625453]
16. Papaioannou J, White A. Maintained activity of lateral geniculate nucleus neurons as a function of background luminance. Exp.Neurol. 1972; 34:558–566. [PubMed: 4336771]
17. Marrocco RT. Possible neural basis for brightness magnitude estimates. Brain Res. 1975; 86:128–133. [PubMed: 1115988]
18. Barlow RB Jr. Verillo R. Brightness sensation in a ganzfeld. Vis. Res. 1976; 16:1291–1297. [PubMed: 1007002]
19. Doty RW. Tonic retinal influences in primates. Ann. New York Acad. Sci. 1977; 290:139–151. [PubMed: 96720]
20. Spear PD, Smith DC, Williams LL. Visual receptive-field properties of single neurons in cat's ventral lateral geniculate nucleus. J. Neurophysiol. 1977; 40:390–409. [PubMed: 845627]
21. Barlow RB Jr. Snodderly DM, Swadlow HA. Intensity coding in primate visual system. Exp. Brain Res. 1978; 31:163–177. [PubMed: 415894]
22. Kayama Y, Riso RR, Bartlett JR, Doty RW. Luxotonic responses of units in macaque striate cortex. J. Neurophysiol. 1979; 42:1495–1517. [PubMed: 115968]
23. Spear PD, Moore RJ, Kim CBY, Xue J-T, Tumosa N. Effects of aging on the primate visual system: Spatial and temporal processing by lateral geniculate neurons in young adult and old rhesus monkeys. J. Neurophysiol. 1994; 72:402–420. [PubMed: 7965023]
24. Van Hooser SD, Alexander J, Heimel F, Nelson SB. Receptive field properties and laminar organization of lateral geniculate nucleus in the gray squirrel (Sciurus carolinesis). J. Neurophysiol. 2003; 90:3398–3418. [PubMed: 12840084]
25. Tucker TR, Fitzpatrick D. Luminance-evoked inhibition in primary visual cortex: A transient veto of simultaneous and ongoing response. Journal of Neuroscience. 2006; 26(52):13537–13547. [PubMed: 17192437]
26. Alitto HJ, Moore BD IV, Rathburn DL, Ursey WM. A comparison of visual responses in the lateral geniculate nucleus of alert and anaesthetized macaque monkeys. J. Physiol. 2011; 589:87–99. [PubMed: 20603332]
27. Albrecht, DG.; Geisler, WS.; Crane, AM. Nonlinear properties of visual cortex neurons: Temporal dynamics, stimulus selectivity, neural performance. In: Chalupa, LM.; Werner, JS., editors. The Visual Neurosciences. Vol. 1. MIT Press; 2003. p. 747-764.
28. Rodieck RW. Quantitative analysis of cat retinal ganglion cell response to visual stimuli. Vis. Res. 1965; 5:583–601. [PubMed: 5862581]
29. Enroth-Cugell C, Robson JG. The contrast sensitivity of retinal ganglion cells of the cat. J. Physiol. (London). 1966; 187:517–552. [PubMed: 16783910]
30. Mante V, Frazor RA, Bonin V, Geisler WS, Carandini M. Independence of luminance and contrast in natural scenes and in the early visual system. Nat. Neurosci. 2005; 8:1690–1697. [PubMed: 16286933]
31. Frazor RA, Geisler WS. Local luminance and contrast in natural images. Vision Res. 2006; 46:1585–1598. [PubMed: 16403546]
32. Carandini M, Heeger DJ. Normalization as a canonical neural computation. Nature Reviews Neuroscience. 2012; 13:51–62.
33. Robson, JG. Neural images: The physiological basis of spatial vision. In: Harris, CS., editor. Visual Coding and Adaptability. Lawrence Erlbaum Associates; Hillsdale, NJ: 1980. p. 177-214.
34. Levitt JB, Schumer RA, Sherman SM, Spear PD, Movshon JA. Visual response properties of neurons in the LGN of normally reared and visually deprived macaque monkeys. J. Neurophysiol. 2001; 85:2111–2129. [PubMed: 11353027]

35. Irvin GE, Casagrande VA, Norton TT. Center/surround relationships of magnocellular, parvocellular, and koniocellular relay cells in primate lateral geniculate nucleus. Vis. Neurosci. 1993; 10:363–373. [PubMed: 8485098]

36. Kremers J, Weiss S. Receptive field dimensions of lateral geniculate cells in the common marmoset (Callithrix jacchus). Vis. Res. 1997; 37:2171–2181. [PubMed: 9578900]

37. White AJR, Solomon SG, Martin PR. Spatial properties of koniocellular cells in the lateral geniculate nucleus of the marmoset Callithrix jacchus. J. Physiol. 2001; 533:519–535. [PubMed: 11389209]

38. O' Keefe LP, Levitt JB, Kiper DC, Shapley RM, Movshon JA. Functional organization of owl monkey lateral geniculate nucleus and visual cortex. J. Neurophysiol. 1998; 80:594–609. [PubMed: 9705453]

39. Xu X, Bonds AB, Casagrande VA. Modeling receptive-field structure of koniocellular, magnocellular, and parvocellular LGN cells in the owl monkey (Aotus trivigatus). Vis. Neurosci. 2002; 19:703–711. [PubMed: 12688666]

40. Cheng H, Chino YM, Smith EL III, Hamamoto J, Yoshida K. Transfer characteristics of lateral geniculate nucleus X neurons in the cat: Effects of spatial frequency and contrast. J. Neurophysiol. 1995; 74:2548–2557. [PubMed: 8747213]

41. Grubb MS, Thompson ID. Quantitative characterization of visual response properties in the mouse dorsal lateral geniculate nucleus. J. Neurophysiol. 2003; 90:3594–3607. [PubMed: 12944530]

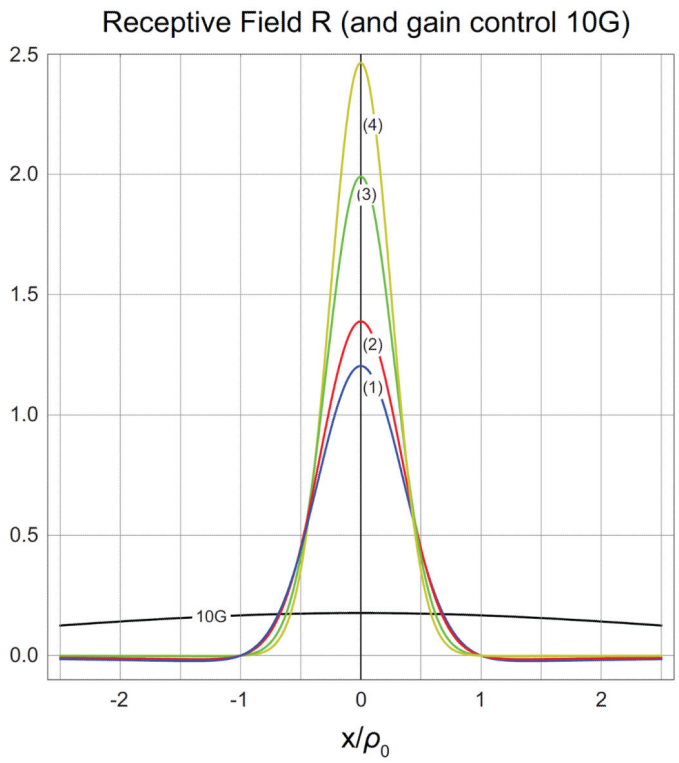

Fig. 1.

Cross-sections of linear field functions R (x_1, 0) vs. x_1/ρ_0 and gain control function $10G$ (x_1, 0) vs. x_1/ρ_0, where ρ_0 is the LGN excitatory center radius (Section 3). Parameter values: (1) σ_C^2, σ_S^2, β_{CS}=0.1292ρ_0^2, 4.651 ρ_0^2, 0.836 (strong band-pass); (2) σ_C^2, σ_S^2, β_{CS}=0.1130 ρ_0^2, 4.070 ρ_0^2, 0.488 (moderate band-pass); (3) σ_C^2, σ_S^2, β_{CS}=0.0798 ρ_0^2, 2.873 ρ_0^2, 0.081 (weak band-pass); (4) σ_C^2, σ_S^2, β_{CS}=0.0646 ρ_0^2, 2.326 ρ_0^2, 0.019 (low-pass); and σ_G^2=9.0 ρ_0^2 (gain control).

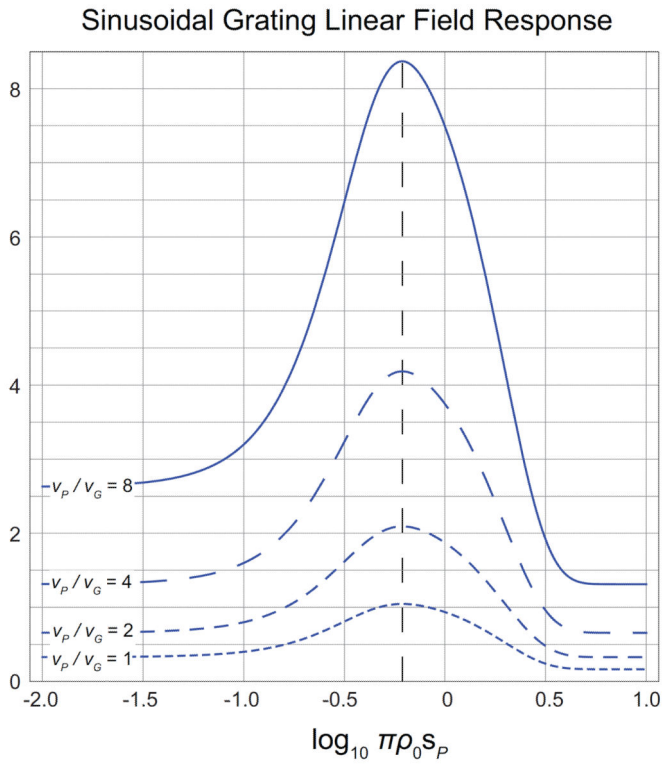

Fig. 2.

Sinusoidal grating linear field response maximum $(R[P]/\nu_G)_{max}$ vs. normalized spatial frequency $\log_{10}(\pi\rho_0 s_P)$ for the strong band-pass case of Fig. 1 and levels SNR = 1 (short dashing), SNR = 2 (medium dashing), SNR = 4 (long dashing), SNR = 8 (solid), at maximum grating contrast, $c_P = 1$. The linear response is scaled by the SNR value, in particular, there is no change in the optimal spatial frequency $\pi\rho_0 s_P = 0.614$ (vertical dashed line) as SNR varies.

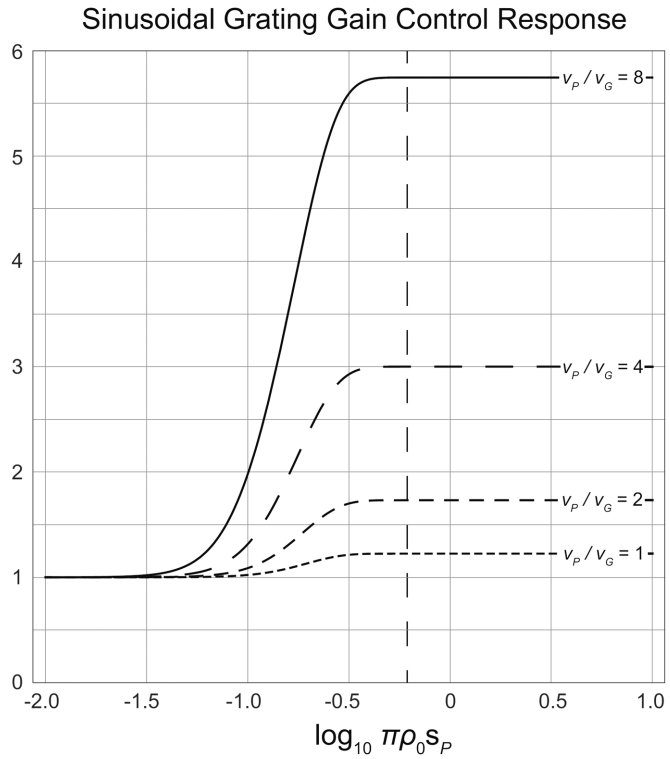

Fig. 3.

Sinusoidal grating gain control response minimum $(G[P]/\nu_G)_{min}$ vs. normalized spatial frequency $\log_{10}(\pi\rho_0 s_P)$ for gain control parameter $\sigma_G^2 = 9\rho_0^2$, contrast $c_P = 1$, and SNR = 1, 2, 4, 8, matching Fig. 2. The gain control response turns from "off" at low frequencies to "on" at higher frequencies. The plateau level is proportional to SNR but is essentially independent of σ_G^2, which determines where the plateau begins. The vertical dashed line marks the linear response optimal spatial frequency $\pi\rho_0 s_P = 0.614$ (Fig. 2).

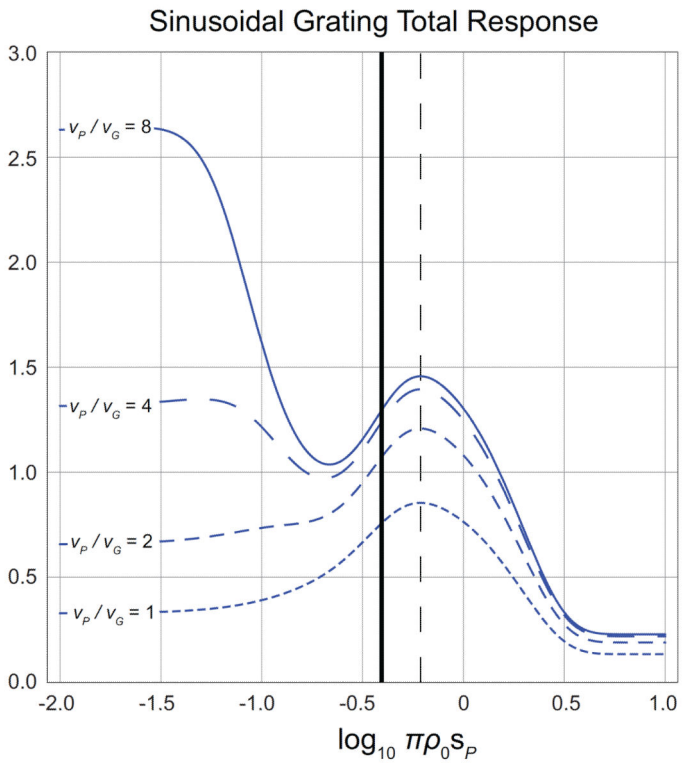

Fig. 4.

Sinusoidal grating total response maximum $\left(\frac{\mathrm{LGN}[P]}{\nu_{\mathrm{LGN}}}\right)_{max}$ vs. normalized spatial frequency $\log_{10}(\pi\rho_0 s_P)$ for the four linear responses of Fig. 2 (strong band-pass case of Fig. 1 at levels SNR = 1 (short dashing), SNR = 2 (medium dashing), SNR = 4 (long dashing), SNR = 8 (solid). The vertical solid line is a nominal boundary where gain control becomes effective at higher frequencies. The vertical dashed line is the linear optimal spatial frequency $\pi\rho_0 s_P = 0.614$. In all cases, gain control is fully effective at the optimal spatial frequency, which remains stable as SNR varies.

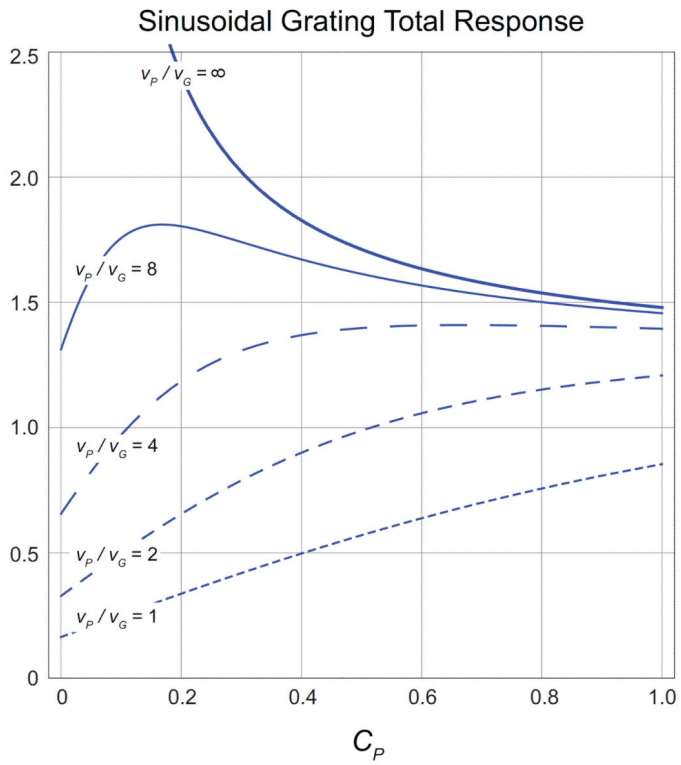

Fig. 5.

Sinusoidal grating total response maximum $\left(\frac{\mathrm{LGN}[P]}{\nu_{\mathrm{LGN}}}\right)_{max}$ vs. contrast c_P for the strong band-pass case of Fig. 1 with spatial frequency at the optimal value ($\pi\rho_0 s_P = 0.614$) and gain parameter $\sigma_G^2 = 9\rho_0^2$. The curves correspond to SNR = 1, 2, 4, 8 and the saturated response limit SNR = ∞. Notice contrast saturation at SNR = 4 and super-saturation at SNR = 8. The model predicts super-saturation in the sinusoidal grating response as a general effect with increasing SNR.

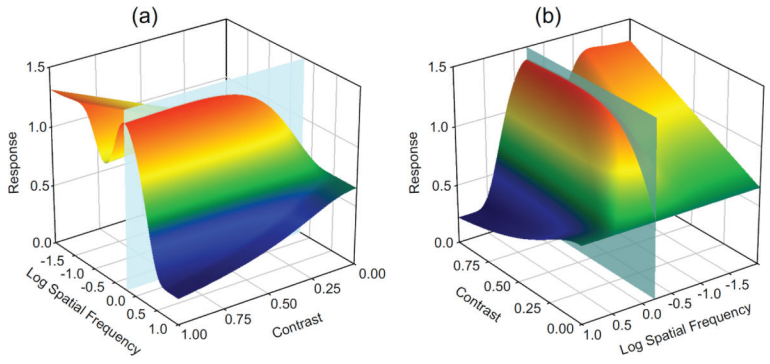

Fig. 6.

Sinusoidal grating total response maximum $\left(\frac{\mathrm{LGN}[P]}{\nu_{\mathrm{LGN}}}\right)_{max}$ for the strong band-pass case of Fig. 1 with gain parameter $\sigma_G^2 = 9\rho_0^2$ and SNR = 4 vs. contrast c_P and normalized spatial frequency $\log_{10}(\pi\rho_0 s_P)$. The contrast saturation curve in Fig. 5 is a cross-section of this plot at the vertical plane marking the optimal spatial frequency ($\pi\rho_0 s_P = 0.614$). Notice the optimal frequency is independent of contrast.